

Address-Event Variable-Length Compression for Time-Encoded Data

Sharu Theresa Jose and Osvaldo Simeone

Abstract—Time-encoded signals, such as social network update logs and spiking traces in neuromorphic processors, are defined by multiple traces carrying information in the timing of events, or spikes. When time-encoded data is processed at a remote site with respect to the location it is produced, the occurrence of events needs to be encoded and transmitted in a timely fashion. The standard Address-Event Representation (AER) protocol for neuromorphic chips encodes the indices of the “spiking” traces in the payload of a packet produced at the same time the events are recorded, hence implicitly encoding the events’ timing in the timing of the packet. This paper investigates the potential bandwidth saving that can be obtained by carrying out variable-length compression of packets’ payloads. Compression leverages both intra-trace and inter-trace correlations over time that are typical in applications such as social networks or neuromorphic computing. The approach is based on discrete-time Hawkes processes and entropy coding with conditional codebooks. Results from an experiment based on a real-world retweet dataset are also provided.

I. INTRODUCTION

Time-encoded information underlies many data types of increasing importance, such as social network update times [1], communication network logs [2], retweet traces [3], wireless activity sensors [4], neuromorphic sensors [5], [6], and synaptic traces from in-brain measurements for brain-computer interfaces [7]. Time-encoded signals are defined by multiple traces, each carrying information in the timing of *events*, also known as spikes (see Figure 1). To elaborate on some examples, neuromorphic cameras encode information by producing a spike in response to changes in the sensed environment [6]; neurons in a Spiking Neural Networks (SNNs) compute and communicate via spiking traces in a way that mimics the operation of biological brains [5], [8]; social networks keep logs of update times for all users [1]; and wireless sensors can measure the activity on given channels as binary (on-off) time-frequency binary maps [4].

When time encoded data is processed at a remote site with respect to the location in which the data is produced, the occurrence of events needs to be encoded and transmitted in a timely fashion. A notable example is given by SNN chips for which neurons are partitioned into several cores, and spikes produced by neurons in a given core need to be conveyed to the recipient neurons in a separate core in order

The authors are with King’s Communications, Learning, and Information Processing (KCLIP) lab at the Department of Engineering of Kings College London, UK (emails: sharu.jose@kcl.ac.uk, osvaldo.simeone@kcl.ac.uk). The authors have received funding from the European Research Council (ERC) under the European Unions Horizon 2020 Research and Innovation Programme (Grant Agreement No. 725731). The authors thank Prof. Rajendran (KCL) for useful discussions.

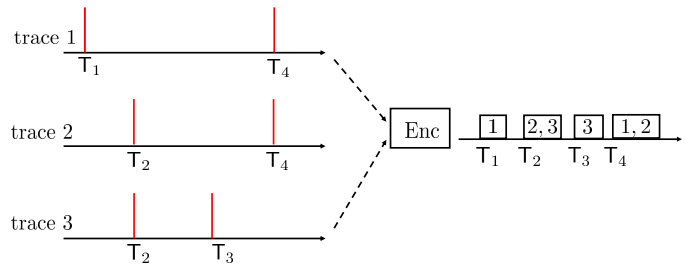


Fig. 1: Illustration of the problem of variable-length address-event compression with $N = 3$ traces: At each events’ occurrence time T_n , the encoder outputs a variable-length packet describing the set \mathcal{I}_n of traces producing an event.

to enable correct processing [8]. If a packet encoding the occurrence of one or more events is produced at the same time (within some tolerance) in which the events take place, then timing information is directly carried by the reception of the packet. Therefore, the packet payload only needs to contain information about the identity, also referred to as “addresses”, of the “spiking” traces. This is the approach taken by the Address Event Representation (AER) protocol, which is the de facto standard for the representation and transmission of time-encoded data in neuromorphic sensors and implementations of SNNs [9]–[11].

This paper studies the problem of compressing packets generated by an AER-like protocol for generic time-encoded data. The key idea is that time-encoded traces are typically characterized by strong correlations both over time and across different traces. For instance, the spike timings in biological neural traces reveal excitatory and inhibitory inter-neuron effects [12]; and the timing of tweets of different users are correlated within chains of retweets [3]. These intra- and inter-trace correlations can be harnessed to compress, using variable-length codes, the description of the identity, or addresses, of the event-producing traces at a given time. Our approach is based on discrete-time Hawkes processes [13] and entropy coding with conditional codebooks [14].

To the best of our knowledge the problem of compression for AER-like protocols has not been studied in the literature. Extensive work has been carried out for the related problems of converting bandlimited or finite-innovation signals into time-encoded information [15], [16]; and of representing point processes as bit streams [17]. There are also active lines of research on the definition and learning of statistical models of point processes as sources of time-encoded information [18], [19]; as well as on the estimation of statistical measures

of correlations within time-encoded data streams, such as Granger causality or directed information [20]. Other related works concern the transmission of time-encoded information over queuing channels that randomly delay input spikes or events [21], [22].

Notation: Throughout this paper, we use upper case sans-serif letters e.g., X , to represent random variables, and upper case letters e.g., X , to represent realizations of the random variables. We use bold sans-serif letters, e.g., \mathbf{X} , to represent random vectors or matrices, and the corresponding upper case letters, e.g., \mathbf{X} , to denote its realization. We also use calligraphic upper case letters e.g., \mathcal{X} , to represent random sets, and the upper case typewriter letter, e.g., \mathbf{X} , to represent a realization. We use the notation $[N] = \{1, \dots, N\}$, and $2^{[N]}$ represents the power set, i.e., the set of all subsets of $[N]$, while $\{\emptyset\}$ represents the empty set. Furthermore, we let \mathbf{D} represent a sparse lower shift matrix with $[\mathbf{D}]_{r,c} = 1(\{r-c=1\})$ where $1(\cdot)$ is the indicator function which takes value 1 when ‘.’ is true and equals zero otherwise. We also use \mathbf{O} to represent an all-zero matrix.

II. PROBLEM FORMULATION

In this section, we present the problem formulation by describing first the probabilistic model of the considered sources and then the address-event compression problem.

A. Multivariate Discrete-Time Hawkes Process

Throughout this paper, as illustrated in Figure 1, we consider time-encoded data defined by N discrete-time traces over time index $t = 1, 2, \dots$. Each trace records the timings of events from a given source, e.g., tweets from a user or spikes from a neuron. Mathematically, we define $X^{(i)}(t) \in \{0, 1\}$ as the random variable that takes value 1 when an event of trace i occurs at time t , and is equal to zero otherwise. Accordingly, the N dimension row vector $\mathbf{X}(t) = (X^{(1)}(t), X^{(2)}(t), \dots, X^{(N)}(t))$ represents the values of all the traces at time t . For each trace $i \in [N]$, we define the time of occurrence of the k th event as

$$T_k^{(i)} = \min \left\{ t : \sum_{t' \leq t} X^{(i)}(t') = k \right\}, \quad (1)$$

and the timing of the n th event across all traces as

$$T_n = \min \left\{ t : \sum_{t' \leq t} 1(\mathbf{X}(t') \neq \mathbf{O}) = n \right\}. \quad (2)$$

Moreover, we use $\mathbf{X}(1:t-1) = (\mathbf{X}(1), \dots, \mathbf{X}(t-1))$ to define the (past) history of traces at time t .

The arrival of events are generally correlated across time and traces, capturing excitation or inhibition effects within a trace and among different traces. To account for these effects, each trace $i \in [N]$ is associated with an intensity function [23] $\lambda^{(i)}(t|\mathbf{X}(1:t-1))$, which depends on the history $\mathbf{X}(1:t-1)$ of all traces as

$$\lambda^{(i)}(t|\mathbf{X}(1:t-1)) = \lambda_i + \sum_{j=1}^N \sum_{k: T_k^{(j)} < t} \nu_{i,j}(t - T_k^{(j)}). \quad (3)$$

In (3), parameter $\lambda_i > 0$ is a baseline intensity; and each function $\{\nu_{i,j}(t)\}_{t \geq 1}$, with $\nu_{i,j}(t) = 0$ for $t < 1$, is known as the kernel function for a pair of traces $i, j \in [N]$. As detailed below, a larger intensity $\lambda^{(i)}(t|\mathbf{X}(1:t-1))$ implies a larger probability for trace i “spiking” at time t . Therefore, when the (i, j) th kernel satisfies $\nu_{i,j}(t') > 0$ for some $t' \geq 1$, the occurrence of an event at trace j at time $t - t'$ increases the intensity of trace i at time t . Conversely, a decrease in the intensity of trace i is caused by the same event if the (i, j) th kernel satisfies $\nu_{i,j}(t') < 0$. Note also that when $\nu_{i,j}(\cdot) \equiv 0$ for all $i, j \in [N]$, the N traces of events are independent of each other, and each trace i follows a discrete-time Poisson process of rate λ_i . A typical example of a kernel is the exponential kernel [23], which is defined as

$$\nu_{i,j}(t) = \alpha_{i,j} \exp(-t/\beta_{i,j}), \quad \text{for } t = 1, 2, \dots, \quad (4)$$

with parameters $\alpha_{i,j}$ and $\beta_{i,j} > 0$ for all pairs of traces $i, j \in [N]$.

Definition 2.1 (Discrete-Time Multivariate Hawkes Process [23]): For a discrete-time N -dimensional Hawkes process $\{\mathbf{X}(t)\}_{t \geq 1}$, the probability of vector $\mathbf{X}(t)$ given the history $\mathbf{X}(1:t-1)$ is given as

$$\begin{aligned} \mathbb{P}[\mathbf{X}(t) = \mathbf{X} | \mathbf{X}(1:t-1) = \mathbf{X}(1:t-1)] \\ = \prod_{i=1}^N \mathbb{P}[X^{(i)}(t) = \mathbf{X}^{(i)} | \mathbf{X}(1:t-1) = \mathbf{X}(1:t-1)], \end{aligned} \quad (5)$$

$$\begin{aligned} \text{where } \mathbb{P}[X^{(i)}(t) = 1 | \mathbf{X}(1:t-1) = \mathbf{X}(1:t-1)] \\ = \sigma(\lambda^{(i)}(t|\mathbf{X}(1:t-1))), \end{aligned} \quad (6)$$

with $\sigma(a) = (1 + e^{-a})^{-1}$ representing the sigmoid function and $\lambda^{(i)}(t|\mathbf{X}(1:t-1))$ being the intensity function in (3).

In this paper, we focus our attention on discrete-time multivariate Hawkes process with finite memory τ . Accordingly, the probability of an event of trace i occurring at any time instant t depends solely on a τ -length history, i.e., on the *state*

$$\mathbf{S}(t) = \mathbf{X}(t-\tau:t-1). \quad (7)$$

Definition 2.2 (Discrete-Time Multivariate τ -Memory Hawkes Process): A discrete-time τ -memory N -dimensional Hawkes process is defined as in (5), (6) and (3) with kernel $\nu_{i,j}(t)$ satisfying $\nu_{i,j}(t) = 0$ for $t > \tau$ and for all $i, j \in [N]$.

In the subsequent sections, we use the notation $\mathcal{S} = \{0, 1\}^{\tau N}$ to denote the set of all $2^{\tau N}$ possible states \mathbf{S} .

B. Address-Event Variable-Length Compression

In order to define the compression problem of interest, we first introduce the *address-event process* for the multivariate Hawkes process introduced above.

Definition 2.3 (Address-Event Process): For a discrete-time τ -memory multivariate Hawkes process $\{\mathbf{X}(t)\}_{t \geq 1}$, the address-event process is defined as the random sequence of

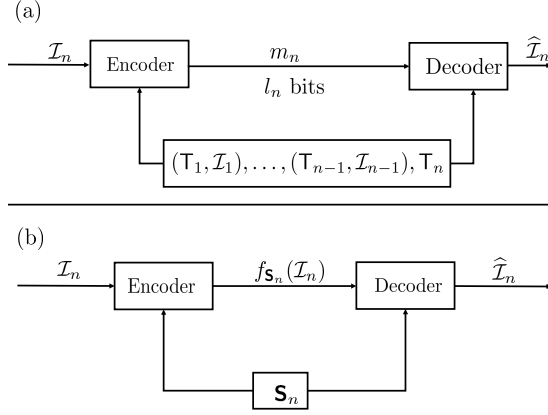


Fig. 2: Address-event variable length compression: (a) original problem, and (b) equivalent formulation.

subsets of indices, or addresses, $\{\mathcal{I}_n\}_{n \geq 1}$, where \mathcal{I}_n is the subset of traces that produce an event at time T_n in (2) as

$$\mathcal{I}_n = \{i \in [N] : X^{(i)}(T_n) = 1\}. \quad (8)$$

We also denote as $\Delta T_n = T_n - T_{n-1}$ the inter-arrival time between two successive event arrivals from any of the traces, with $T_0 = 0$.

As illustrated in Figure 1, we focus on address-event communication protocols motivated by AER [10], [24]. Accordingly, at any time T_n , the protocol produces a packet describing the index set \mathcal{I}_n of the traces, or addresses, of the events occurring at time T_n . Importantly, each packet implicitly carries information about the time T_n in its transmission time, and hence only the subset \mathcal{I}_n needs to be explicitly encoded in the payload of the packet.

To elaborate, consider the n th arrival time T_n . At this point in time, assuming lossless compression, as illustrated in Figure 2(a), the receiver is informed about the previous pairs $\{T_{n'}, \mathcal{I}_{n'}\}_{n' \leq n-1}$, and, thanks to the timing of the current packet, also of the current arrival time T_n . As a result, the decoder can reconstruct the state vector

$$\mathbf{S}_n \triangleq \mathbf{S}(T_n) = \mathbf{X}(T_n - \tau : T_n - 1). \quad (9)$$

We recall that the state (7) summarizes the entire history of the multivariate τ -memory Hawkes Process, yielding the conditional distribution of the set \mathcal{I}_n through (5) and (6). Given that the state \mathbf{S}_n is known to both encoder and the decoder, encoding and decoding functions used to encode and decode the packet produced at any time T_n can be defined to depend on the state \mathbf{S}_n as illustrated in Figure 2(b) and detailed next.

Definition 2.4: An address-event variable-length code $\{f_{\mathbf{S}}, g_{\mathbf{S}}\}_{\mathbf{S} \in \mathcal{S}}$ consists of

- an encoding function $f_{\mathbf{S}}$ that, for each state $\mathbf{S} \in \mathcal{S}$, maps an index set $\mathbf{I} \in 2^{[N]}/\{\emptyset\}$ into a binary string $f_{\mathbf{S}}(\mathbf{I})$ of length $l_{\mathbf{S}}(\mathbf{I})$ bits;
- and a decoding function $g_{\mathbf{S}}$ that, given the state \mathbf{S} and the encoded message, recovers an estimate $\hat{\mathbf{I}} = g_{\mathbf{S}}(f_{\mathbf{S}}(\mathbf{I})) \in 2^{[N]}/\{\emptyset\}$.

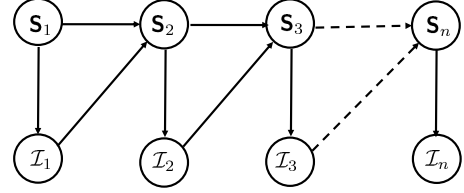


Fig. 3: A Bayesian network representation of the address-event process in Theorem 3.1. Note that, conditioned on the present state \mathbf{S}_n , the index set \mathcal{I}_n is independent of all past index sets $\mathcal{I}_1, \dots, \mathcal{I}_{n-1}$.

A code is said to be lossless if the equality $g_{\mathbf{S}}(f_{\mathbf{S}}(\mathbf{I})) = \mathbf{I}$ holds for all subsets $\mathbf{I} \in 2^{[N]}/\{\emptyset\}$ and states $\mathbf{S} \in \mathcal{S}$. For a lossless code, let $\mathbb{C}(\mathbf{S}) = \{f_{\mathbf{S}}(\mathbf{I}) : \mathbf{I} \in 2^{[N]}/\{\emptyset\}\}$ represent the codebook corresponding to state \mathbf{S} . The expected length of the codewords in $\mathbb{C}(\mathbf{S})$ is given by the average

$$L(\mathbf{S}) = \mathbb{E}[l_{\mathbf{S}}(\mathcal{I}) | \mathbf{S}], \quad (10)$$

which is taken with respect to the distribution of \mathcal{I} conditioned on the state \mathbf{S} . A rate R in *bits per event* is said to be achievable if there exists a lossless code for which the following limit holds

$$\limsup_{T \rightarrow \infty} \frac{\sum_{n=1}^{N(T)} L(\mathbf{S}_n)}{N(T)} = R \quad \text{a.s.}, \quad (11)$$

where $N(T) = \max\{n : T_n \leq T\}$ represents the total number of events occurred in the interval $[1, T]$. We are interested in characterizing the infimum R^* of all achievable rates.

III. DISTRIBUTION OF THE ADDRESS-EVENT PROCESS

In this section, we derive the joint distribution of the address-event process and of the state sequence $\{\mathcal{I}_n, \mathbf{S}_n\}_{n \geq 1}$, as well as the marginal distribution of the states $\{\mathbf{S}_n\}_{n \geq 1}$. These results will be instrumental in characterizing the rates (11) as detailed in the next section. To start, we define the following conditional probability distributions (CPDs).

First, we consider the CPD $\mathbb{P}[\mathcal{I}_n = \mathbf{I} | \mathbf{S}_n = \mathbf{S}]$ of a non-empty subset $\mathcal{I}_n = \mathbf{I} \subseteq [N]$ of traces having events' occurrences at time T_n given state $\mathbf{S}_n = \mathbf{S}$. This is needed to evaluate the conditional average rate (10). By (5), the events' occurrences are conditionally independent across traces given the current state, and hence the above CPD evaluates to

$$\mathbb{P}[\mathcal{I}_n = \mathbf{I} | \mathbf{S}_n = \mathbf{S}] = \frac{\prod_{i \in \mathbf{I}} \sigma(\lambda_n^{(i)}(\mathbf{S})) \prod_{j \in \mathbf{I}^c} (1 - \sigma(\lambda_n^{(j)}(\mathbf{S})))}{1 - \prod_{j \in [N]} (1 - \sigma(\lambda_n^{(j)}(\mathbf{S})))}, \quad (12)$$

where $\mathbf{I}^c = [N]/\mathbf{I}$ is the complement set of \mathbf{I} and the intensity

$$\lambda_n^{(i)}(\mathbf{S}) \triangleq \lambda^{(i)}(T_n | \mathbf{S}), \quad \text{for } i \in [N], \quad (13)$$

is as defined in (3). In (12), the numerator corresponds to the probability that only addresses in \mathbf{I} have event occurrences at T_n , while the denominator evaluates the probability that at least one event occurs at time T_n .

Second, for a given inter-arrival time $\Delta T_{n+1} = T_{n+1} - T_n = \Delta T$, the state \mathbf{S}_{n+1} can be evaluated as a deterministic function of the previous state \mathbf{S}_n and index set \mathcal{I}_n as

$$\mathbf{S}_{n+1} = \eta(\Delta T, \mathbf{S}_n, \mathcal{I}_n), \quad (14)$$

$$\text{with } \eta(\Delta T, \mathbf{S}_n, \mathbf{I}) = \mathbf{D}^{\Delta T-1} \left(\mathbf{D} \mathbf{S}_n + \mathbf{I}(\mathbf{I}) \right), \quad (15)$$

and $\mathbf{I}(\mathbf{I})$ representing a $\tau \times N$ matrix with $[\mathbf{I}(\mathbf{I})]_{r,c} = 1$ ($\{r = 1\}$ and $\{c \in \mathbf{I}\}$). To see why (14)-(15) hold, note that each time instant with no events causes the state matrix to shift down by one unit with a new all-zero row (no event) added on top, yielding the matrix $\mathbf{D} \mathbf{S}_n$; while events recorded at traces in subset $\mathcal{I}_n = \mathbf{I}$ modify the state \mathbf{S}_{n+1} by adding matrix $\mathbf{I}(\mathbf{I})$. Using this observation together with the conditional independence of events of traces at a time given the current state as per (5), we have the CPD for the inter-arrival times

$$\begin{aligned} & \mathbb{P}[\Delta T_{n+1} = \Delta T | \mathbf{S}_n = \mathbf{S}, \mathcal{I}_n = \mathbf{I}] \\ &= \left(\prod_{i \in [N]} \prod_{j=1}^{\Delta T-1} \left(1 - \sigma(\lambda_n^{(i)}(\eta(j, \mathbf{S}, \mathbf{I}))) \right) \right) \times \\ & \quad \left(1 - \prod_{i \in [N]} \left(1 - \sigma(\lambda_n^{(i)}(\eta(\Delta T, \mathbf{S}, \mathbf{I}))) \right) \right). \end{aligned} \quad (16)$$

The first of the product terms in (16) evaluates the probability that no events from any of the traces occur during the times $T_n + 1, \dots, T_n + \Delta T - 1$, and the second term similarly computes the probability that at least one event of a trace occurs at time T_{n+1} . From these two observations, the joint probability distribution of $\{\mathcal{I}_n, \mathbf{S}_n\}_{n \geq 1}$ is characterized as follows.

Theorem 3.1: The joint distribution of the address-event process and state sequence $\{\mathcal{I}_n, \mathbf{S}_n\}_{n \geq 1}$ factorizes as

$$\begin{aligned} \mathbb{P}\{\{\mathcal{I}_n, \mathbf{S}_n\}_{n \geq 1}\} &= \mathbb{P}\{\mathbf{S}_1\} \prod_{n \geq 1} \mathbb{P}\{\mathbf{S}_{n+1}, \mathcal{I}_n | \mathbf{S}_n\} \\ &= \mathbb{P}\{\mathbf{S}_1\} \prod_{n \geq 1} \mathbb{P}\{\mathcal{I}_n | \mathbf{S}_n\} \mathbb{P}\{\mathbf{S}_{n+1} | \mathcal{I}_n, \mathbf{S}_n\}, \end{aligned} \quad (17)$$

where $\mathbb{P}\{\mathbf{S}_1\} = \mathbb{P}[\Delta T_1 | \mathbf{S}_0 = \mathbf{O}, \mathcal{I}_0 = \{\emptyset\}]$ with $\mathbb{P}\{\mathbf{S}_1 = \mathbf{O}\} = 1$, the CPD $\mathbb{P}\{\mathcal{I}_n | \mathbf{S}_n\}$ is as given in (12) and we have the CPD

$$\begin{aligned} & \mathbb{P}\{\mathbf{S}_{n+1} = \mathbf{S}_{n+1} | \mathcal{I}_n = \mathbf{I}, \mathbf{S}_n = \mathbf{S}\} = \\ & \begin{cases} \mathbb{P}[\Delta T_{n+1} = \Delta T | \mathcal{I}_n = \mathbf{I}, \mathbf{S}_n = \mathbf{S}] & \text{if } \mathbf{S}_{n+1} = \eta(\Delta T, \mathbf{S}, \mathbf{I}) \\ & \text{and } 1 \leq \Delta T \leq \tau, \\ 1 - \sum_{\Delta T=1}^{\tau} \mathbb{P}[\Delta T_{n+1} = \Delta T | \mathcal{I}_n = \mathbf{I}, \mathbf{S}_n = \mathbf{S}] & \text{if } \mathbf{S}_{n+1} = \mathbf{O}, \\ 0 & \text{otherwise,} \end{cases} \end{aligned} \quad (18)$$

with $\mathbb{P}[\Delta T_{n+1} | \mathcal{I}_n = \mathbf{I}, \mathbf{S}_n = \mathbf{S}]$ given in (16).

According to Theorem 3.1, the joint distribution of the pairs $\{\mathcal{I}_n, \mathbf{S}_n\}_{n \geq 1}$ factorizes according to the Bayesian network [25] in Figure 3. As a corollary, it follows that the system states \mathbf{S}_n evolves as a Markov chain, as detailed next.

Corollary 3.2: The evolution of system states $\{\mathbf{S}_n\}_{n \geq 1}$ forms a Markov chain such that

$$\mathbb{P}\{\mathbf{S}_{n+1} | \mathbf{S}_1, \dots, \mathbf{S}_n\} = \mathbb{P}\{\mathbf{S}_{n+1} | \mathbf{S}_n\},$$

with the transition probability

$$\begin{aligned} & \mathbb{P}\{\mathbf{S}_{n+1} = \mathbf{S}_{n+1} | \mathbf{S}_n = \mathbf{S}\} = \\ & \begin{cases} \mathbb{P}[\Delta T_{n+1} = \Delta T, \mathcal{I}_n = \mathbf{I}, | \mathbf{S}_n = \mathbf{S}] & \text{if } \mathbf{S}_{n+1} = \eta(\Delta T, \mathbf{S}, \mathbf{I}) \\ & \text{for } \mathbf{I} \in 2^{[N]} / \{\emptyset\}, \\ & \text{and } 1 \leq \Delta T \leq \tau, \\ 1 - \sum_{\Delta T=1}^{\tau} \sum_{\mathbf{I} \in 2^{[N]} / \{\emptyset\}} \mathbb{P}[\Delta T_{n+1} = \Delta T, \mathcal{I}_n = \mathbf{I} | \mathbf{S}_n = \mathbf{S}] & \text{if } \mathbf{S}_{n+1} = \mathbf{O}, \\ 0 & \text{otherwise,} \end{cases} \end{aligned} \quad (19)$$

where $\mathbb{P}\{\mathcal{I}_n | \mathbf{S}_n\}$ and $\mathbb{P}[\Delta T_{n+1} | \mathcal{I}_n, \mathbf{S}_n]$ are as given in (12) and (16). Moreover, the above Markov chain is irreducible, and there exists a unique $|\mathcal{S}| \times 1$ dimension stationary distribution $\boldsymbol{\pi}$ as the solution of the linear system $\mathbf{P} \boldsymbol{\pi} = \boldsymbol{\pi}$, where $\mathbf{P} = \{\mathbb{P}\{\mathbf{S}_{n+1} = \mathbf{S}' | \mathbf{S}_n = \mathbf{S}\}\}_{\mathbf{S}, \mathbf{S}' \in \mathcal{S}}$ is the transition matrix.

Proof: See Appendix A. \blacksquare

IV. MINIMUM RATE

In this section, based on the key results reported above, we derive the minimum compression rate R^* in bits per event for the address-event compression problem defined in Section II-B. To this end, we first obtain a general expression for the achievable rate R defined in (11) as a function of the CPD (12) and of the stationary state distribution derived in Corollary 3.2.

Lemma 4.1: The rate R achievable by a lossless address-event variable length code $\{f_{\mathbf{S}}, g_{\mathbf{S}}\}_{\mathbf{S} \in \mathcal{S}}$ defined in (11) equals

$$R = \mathbb{E}_{\boldsymbol{\pi}}[L(\mathbf{S})], \quad (20)$$

where $\boldsymbol{\pi}$ is the stationary distribution of the Markov process $\{\mathbf{S}_n\}_{n \geq 1}$ as defined in Corollary 3.2.

Proof: See Appendix B. \blacksquare

Based on Lemma 4.1, the infimum R^* of all achievable rates can be obtained by applying for each state $\mathbf{S} \in \mathcal{S}$ the variable-length code $\mathbb{C}(\mathbf{S})$ that yields the minimum expected length, as derived in [26]. Specifically, for each state value $\mathbf{S} \in \mathcal{S}$, we order the address sets $\mathbf{I} \in 2^{[N]} / \{\emptyset\}$ in decreasing order of their conditional probabilities $\mathbb{P}\{\mathcal{I} = \mathbf{I} | \mathbf{S} = \mathbf{S}\}$, breaking ties in a lexicographical ordering on $2^{[N]} / \{\emptyset\}$. Codewords are then assigned from the shortest ('0' and '1') to progressively longer ones in this order. Mathematically, let

$$r_{\mathbf{S}} : 2^{[N]} / \{\emptyset\} \rightarrow \{1, 2, \dots, 2^N - 1\} \quad (21)$$

denote an indexing function such that $r_{\mathbf{S}}(\mathbf{I}_1) < r_{\mathbf{S}}(\mathbf{I}_2)$ if $\mathbb{P}\{\mathcal{I} = \mathbf{I}_1 | \mathbf{S} = \mathbf{S}\} > \mathbb{P}\{\mathcal{I} = \mathbf{I}_2 | \mathbf{S} = \mathbf{S}\}$ or if $\mathbb{P}\{\mathcal{I} = \mathbf{I}_1 | \mathbf{S} = \mathbf{S}\} = \mathbb{P}\{\mathcal{I} = \mathbf{I}_2 | \mathbf{S} = \mathbf{S}\}$ and \mathbf{I}_1 precedes \mathbf{I}_2 in lexicographical order. The code $\mathbb{C}(\mathbf{S})$ assigns to each $\mathbf{I} \in 2^{[N]} / \{\emptyset\}$, a codeword of length $l_{\mathbf{S}}(\mathbf{I}) = \lceil \log_2(r_{\mathbf{S}}(\mathbf{I})/2 + 1) \rceil$ [26].

Theorem 4.1: The optimal compression rate R^* is given as

$$R^* = \mathbb{E}_{\boldsymbol{\pi}}[\mathbb{E}_{\mathcal{I}}[\lceil \log_2(r_{\mathbf{S}}(\mathcal{I})/2 + 1) \rceil] | \mathbf{S}], \quad (22)$$

where function $r_{\mathbf{S}}(\cdot)$ is defined in (21), and the expectation is taken with respect to CPD $\mathbb{P}\{\mathcal{I} | \mathbf{S}\}$ defined in (12).

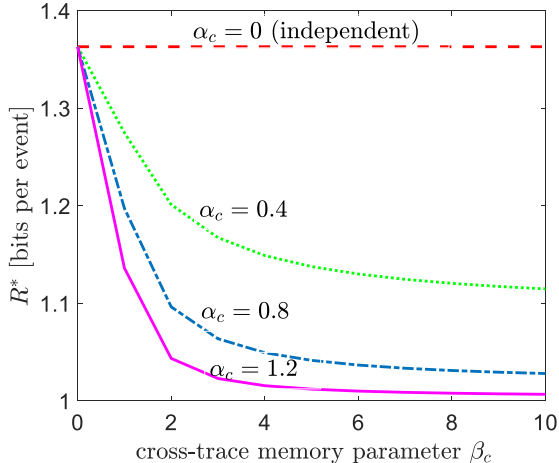


Fig. 4: Optimal rate R^* , in bits per event, versus the cross-trace memory parameter $\beta_c (= \beta_{i,j}, i \neq j)$ for $N = 3$ traces, $\tau = 2$, and the exponential kernel in (4). We consider varying values of cross-trace correlation parameter $\alpha_c (= \alpha_{i,j}, i \neq j)$, and other parameters are set as $\lambda_1 = \lambda_2 = \lambda_3 = 0.4$, $\alpha_{i,i} = 0.95$, $\beta_{i,i} = 3$ for $i \in [N]$.

Figure 4 illustrates the optimal rate R^* in (22), measured in number of bits per event, for $N = 3$ traces as a function of the cross-trace memory parameter $\beta_c = \beta_{i,j}$, for $i \neq j$ and $i, j \in [N]$, for the truncated exponential kernel in (4) with $\tau = 2$. We also vary parameters $\alpha_c = \alpha_{i,j}, i \neq j$, which determine the strength of the correlation across the two traces of events. Note that when $\alpha_c = 0$, the traces are mutually independent, with each following a discrete-time univariate Hawkes process. Other parameters are set as $\lambda_1 = \lambda_2 = \lambda_3 = 0.4$, $\alpha_{i,i} = 0.95$, $\beta_{i,i} = 3$ for $i \in [N]$. A conventional system that does not carry out compression would require a number of bits per event equal to $\log_2(2^N - 1) \approx 2.8$. As seen in Figure 4, the proposed variable-length compression scheme can significantly reduce the average packet length. The rate reduction is particularly pronounced as either α_c increases, so that the correlation between the traces of events strengthens; or as β_c increases, which enhances the dependence of present events of a trace on the past occurrences of the other traces.

V. EXPERIMENT ON REAL-WORLD DATASET

In this section, we implement the proposed variable-length compression scheme on the retweet dataset [18]. The dataset consists of retweet sequences, each corresponding to the retweets of an original tweet. Each retweet event in a sequence is marked with the type of user group (‘small’, ‘medium’ or, ‘large’) and with the time (quantized to an integer) elapsed since the original tweet. Accordingly, each sequence can be formatted into $N = 3$ discrete-time traces. For our experiments, we sampled 2100 sequences from the data set with 2000 sequences used for training and 100 for testing. The training set is used to fit the parameters $\{\lambda_i, \alpha_{i,j}\}_{i,j \in [N]}$ of the Hawkes process with truncated exponential kernel in (4) having fixed memory parameters $\beta_{i,j} = \beta_{i,i} = \beta = 40$, $i, j \in [N]$ and varying τ . This is done by maximizing the training set

log-likelihood, where the likelihood of each sequence is given by (17), via gradient descent log-likelihood estimation [27]. Apart from the described scheme that considers both inter- and intra-trace correlations, for reference, we also consider two simplified strategies: “compression with an i.i.d model” which assumes the traces to be independent (i.e., $\alpha_{i,j} = 0$ for $i, j \in [N], i \neq j$) and memoryless (i.e., $\beta = 0$); and “compression with intra-trace correlation”, which assumes independent traces (i.e., $\alpha_{i,j} = 0$ for $i, j \in [N], i \neq j$) that are allowed to correlate across time. After training, the test sequences are used to evaluate the average number of bits per event, using the trained variable-length code described in Section IV.

As discussed before, without compression, the required rate would be ≈ 2.8 bits per event. As can be seen from Figure 5, compression with an i.i.d model requires only 1.22 bits per event, a gain of 57% over no-compression. Further reductions in rates result from compression schemes that assume intra-trace correlation across time, particularly if accounting also for inter-trace correlations.

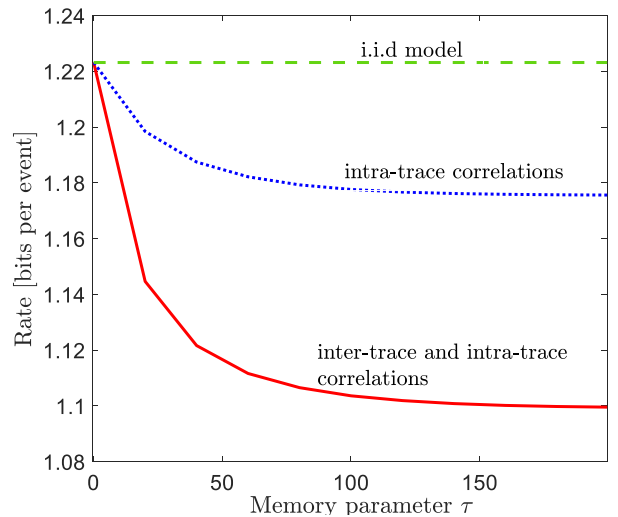


Fig. 5: Rate (in bits per event) versus the system memory parameter τ for the retweet dataset using variable-length compressors trained using Hawkes processes that accounts for no, either, or both intra-trace and inter-trace correlations.

VI. CONCLUSIONS

This paper has considered the problem of timely communication of generic time-encoded data comprising of multiple traces of timings of events. Adhering to the AER communication protocol, whereby the timing of events is implicitly encoded in the packets’ transmission times, we have proposed the use of variable-length compression to reduce the average packet length by leveraging the correlation of the time-encoded data across time and traces. Future works include exploring avenues to reduce the storage complexity of the compression scheme, which requires storing 2^{τ^N} codebooks. One promising solution is to employ a universal approximator, such as a neural network, to output the conditional probabilities $\mathbb{P}[\mathcal{I}|\mathbf{S}]$ as a function of the state \mathbf{S} . Another interesting extension

would be to account for timeout errors resulting in packet dropouts or erasures, which has implications for neuromorphic chips [28].

APPENDIX A PROOF OF COROLLARY 3.2

It follows from Theorem 3.1 that the CDP at hand is obtained through the marginalization

$$\begin{aligned} & \mathbb{P}[\mathbf{S}_{n+1} = \mathbf{S}_{n+1} | \mathbf{S}_n = \mathbf{S}] \\ &= \sum_{\mathcal{I} \in 2^{[N]} / \{\emptyset\}} \mathbb{P}[\mathcal{I}_n = \mathcal{I} | \mathbf{S}_n = \mathbf{S}] \mathbb{P}[\mathbf{S}_{n+1} = \mathbf{S}_{n+1} | \mathcal{I}_n = \mathcal{I}, \mathbf{S}_n = \mathbf{S}]. \end{aligned} \quad (23)$$

However, from (15), as long as we have $\Delta T_{n+1} \in \{1, \dots, \tau\}$, the state $\mathbf{S}_{n+1} = \eta(\Delta T_{n+1}, \mathbf{S}, \mathcal{I}_n)$ assumes a distinct value for each $\mathcal{I}_n = \mathcal{I} \in 2^{[N]} / \{\emptyset\}$. Therefore, the summation over index sets in (23) reduces to the unique index set that produces the state \mathbf{S}_{n+1} . This results in the transition probability corresponding to the first case in (19). Moreover, given the previous state $\mathbf{S}_n = \mathbf{S}$, \mathbf{S}_{n+1} can reach the all-zero state \mathbf{O} with any index set $\mathcal{I}_n = \mathcal{I} \in 2^{[N]} / \{\emptyset\}$ when we have $\Delta T_{n+1} > \tau$. Consequently, the summation in (23) yields the second case of (19).

Given the previous state $\mathbf{S}_n = \mathbf{S}$, there exists $\tau(2^N - 1)$ distinct states that \mathbf{S}_{n+1} can visit, excluding the all-zero state. Therefore, the set of all possible states form one closed communicating class, and the chain is irreducible. Moreover, this set is of finite cardinality, i.e., $|\mathcal{S}| = 2^{\tau N}$. Consequently, the Markov sequence $\{\mathbf{S}_n\}_{n \geq 1}$ has a unique stationary distribution.

APPENDIX B PROOF OF LEMMA 4.1

For any lossless code $\{f_{\mathbf{S}}, g_{\mathbf{S}}\}_{\mathbf{S} \in \mathcal{S}}$, the rate (11) can be written as

$$\frac{\sum_{n=1}^{N(T)} L(\mathbf{S}_n)}{N(T)} = \sum_{\mathbf{S} \in \mathcal{S}} L(\mathbf{S}) \frac{\sum_{n=1}^{N(T)} \mathbb{I}\{\mathbf{S}_n = \mathbf{S}\}}{N(T)},$$

where $\sum_{n=1}^{N(T)} \mathbb{I}\{\mathbf{S}_n = \mathbf{S}\} / N(T)$ measures the fraction of visits to state \mathbf{S} by the Markov process $\{\mathbf{S}_n\}_{n \geq 1}$ in a total of $N(T)$ event occurrence times. It then follows from the strong law of large numbers that the limit

$$\limsup_{T \rightarrow \infty} \frac{\sum_{n=1}^{N(T)} \mathbb{I}\{\mathbf{S}_n = \mathbf{S}\}}{N(T)} \rightarrow \pi(\mathbf{S}) \quad \text{a.s.},$$

holds, which yields (20).

REFERENCES

- [1] C. Dwyer, S. Hiltz, and K. Passerini, "Trust and privacy concern within social networking sites: A comparison of facebook and myspace," *Proc. of AMCIS 2007, Keystone, Colorado*, p. 339, Aug. 2007.
- [2] D. Takahashi and Y. Xiao, "Retrieving knowledge from auditing log-files for computer and network forensics and accountability," *Security and Communication Networks*, vol. 1, no. 2, pp. 147–160, Mar. 2008.
- [3] Q. Zhao, M. A. Erdogdu, H. Y. He, A. Rajaraman, and J. Leskovec, "Seismic: A self-exciting point process model for predicting tweet popularity," in *Proc. of ACM SIGKDD Int. Conf. Knowledge Discovery and Data Mining, Sydney, Australia*, Aug. 2015, pp. 1513–1522.
- [4] T. Endo and T. Fujii, "Real time information gathering based on frequency and timing assignment for wireless sensor networks," in *Proc. of 2012 IEEE Int. Conf. Communication Systems (ICCS), Singapore*, Nov. 2012, pp. 167–171.
- [5] O. Simeone, B. Rajendran, A. Gruning, E. S. Eleftheriou, M. Davies, S. Deneve, and G.-B. Huang, "Learning algorithms and signal processing for brain-inspired computing [from the guest editors]," *IEEE Signal Processing Magazine*, vol. 36, no. 6, pp. 12–15, Nov. 2019.
- [6] S.-C. Liu, B. Rueckauer, E. Ceolini, A. Huber, and T. Delbruck, "Event-driven sensing for efficient perception: Vision and audition algorithms," *IEEE Signal Processing Magazine*, vol. 36, no. 6, pp. 29–37, Nov. 2019.
- [7] E. Musk, "An integrated brain-machine interface platform with thousands of channels," *Journal of Medical Internet Research*, vol. 21, no. 10, p. e16194, 2019.
- [8] M. Davies, N. Srinivasa, T.-H. Lin, G. China, Y. Cao, S. H. Choday, G. Dimou, P. Joshi, N. Imam, S. Jain *et al.*, "Loihi: A neuromorphic manycore processor with on-chip learning," *IEEE Micro*, vol. 38, no. 1, pp. 82–99, Feb. 2018.
- [9] M. Mahowald, *An Analog VLSI System for Stereoscopic Vision*. Springer Science & Business Media, 1994, vol. 265.
- [10] K. A. Boahen, "Point-to-point connectivity between neuromorphic chips using address events," *IEEE Trans. Circuits and Systems II: Analog and Digital Signal Processing*, vol. 47, no. 5, pp. 416–434, May 2000.
- [11] C. M. Higgins and C. Koch, "Multi-chip neuromorphic motion processing," in *Proc. of IEEE Conference on Advanced Research in VLSI, Atlanta, USA*, Mar. 1999, pp. 309–323.
- [12] P. Dayan and L. F. Abbott, *Theoretical neuroscience*. Cambridge, MA: MIT Press, 2001, vol. 806.
- [13] Y. Seol, "Limit theorems for discrete Hawkes processes," *Statistics & Probability Letters*, vol. 99, pp. 223–229, Apr. 2015.
- [14] T. M. Cover and J. A. Thomas, *Elements of Information Theory, 2nd Edition*. Wiley-Interscience, Jul. 2006.
- [15] A. A. Lazar and L. T. Tóth, "Perfect recovery and sensitivity analysis of time encoded bandlimited signals," *IEEE Trans. on Circuits and Systems I: Regular Papers*, vol. 51, no. 10, pp. 2060–2073, Oct. 2004.
- [16] R. Alexandru and P. L. Dragotti, "Time-based sampling and reconstruction of non-bandlimited signals," in *Proc. 2019 IEEE Int. Conf. Acoustics, Speech and Signal Processing (ICASSP), Brighton, UK*, May 2019, pp. 7948–7952.
- [17] A. Lapidith, A. Malär, and L. Wang, "Covering point patterns," *IEEE Tran. on Inform. Theory*, vol. 61, no. 9, pp. 4521–4533, Sept. 2015.
- [18] H. Mei and J. M. Eisner, "The neural Hawkes process: A neurally self-modulating multivariate point process," in *Proc. of Advances in Neural Information Processing Systems, Long Beach, CA, USA*, Dec. 2017, pp. 6754–6764.
- [19] Q. Zhang, A. Lipani, O. Kirnap, and E. Yilmaz, "Self-attentive Hawkes processes," *arXiv preprint arXiv:1907.07561*, 2019.
- [20] H. Xu, M. Farajtabar, and H. Zha, "Learning Granger causality for Hawkes processes," in *Proc. of Int. Conf. Machine Learning, New York City, NY, USA*, Jun. 2016, pp. 1717–1726.
- [21] V. Anantharam and S. Verdu, "Bits through queues," *IEEE Trans. Inform. Theory*, vol. 42, no. 1, pp. 4–18, Jan. 1996.
- [22] T. P. Coleman, N. Kiyavash, and V. G. Subramanian, "The rate-distortion function of a poisson process with a queuing distortion measure," in *Proc. of IEEE Data Compression Conference, Washington DC, USA*, Mar. 2008, pp. 63–72.
- [23] P. J. Laub, T. Taimre, and P. K. Pollett, "Hawkes processes," *arXiv preprint arXiv:1507.02822*, 2015.
- [24] M. A. Sivilotti, "Wiring considerations in analog VLSI systems, with application to field-programmable networks," Ph.D. dissertation, California Institute of Technology Pasadena, CA, 1991.
- [25] C. Boutilier, N. Friedman, M. Goldszmidt, and D. Koller, "Context-specific independence in bayesian networks," in *Proc. Int. Conf. Uncertainty in Artificial Intelligence, Oregon, USA*, Aug. 1996, pp. 115–123.
- [26] C. Blundo and R. De Prisco, "New bounds on the expected length of one-to-one codes," *IEEE Trans. Inform. Theory*, vol. 42, no. 1, pp. 246–250, Jan 1996.
- [27] H. Jang, O. Simeone, B. Gardner, and A. Gruning, "An introduction to probabilistic spiking neural networks," *IEEE Signal Processing Magazine*, vol. 36, no. 6, pp. 64–77, Nov. 2019.
- [28] Y. Sakai, B. U. Pedroni, S. Joshi, S. Tanabe, A. Akinin, and G. Cauwenberghs, "Dropout and dropoutnet for reliable neuromorphic inference under communication constraints in network connectivity," *IEEE Journ.*

Emerging and Selected Topics in Circuits and Systems, vol. 9, no. 4, pp. 658–667, Dec. 2019.